

Large-scale aerosol source apportionment in Amazonia

Paulo Artaxo,¹ Eduardo T. Fernandes,¹ José V. Martins,¹ Márcia A. Yamasoe,¹
Peter V. Hobbs,² Willy Maenhaut,³ Karla M. Longo,¹ and Andrea Castanho¹

Abstract. Aerosol particles were collected aboard two Brazilian Bandeirante EMB 110 planes, and the University of Washington Convair C-131A aircraft during the Smoke, Clouds, and Radiation–Brazil (SCAR-B) field project in the Amazon Basin in August and September 1995. Aerosols were collected on Nuclepore and Teflon filters. Aerosol size distribution was measured with a MOUDI cascade impactor. Sampling was performed mostly over areas heavily influenced by biomass burning smoke. Particle-induced X ray emission (PIXE) was used to measure concentrations of up to 20 elements (Al, Si, P, S, Cl, K, Ca, Ti, V, Cr, Mn, Fe, Ni, Cu, Zn, Br, Rb, Sr, Zr, and Pb). Black carbon (BC) and gravimetric mass analysis were also performed. Instrumental neutron activation analysis (INAA) determined the concentrations of about 15 elements on the Teflon filters. Electron probe X ray microanalysis (EPMA) was used to analyze individual aerosol particles. The average aerosol mass concentration was $105 \mu\text{g m}^{-3}$, with a maximum of $297 \mu\text{g m}^{-3}$. Black carbon (BC) averaged $5.49 \mu\text{g m}^{-3}$, or 1–7% of the aerosol mass load. Five aerosol components were revealed by absolute principal factor analysis: (1) a biomass burning component (responsible for 54% of the aerosol mass and associated with BC, K, Cl, Zn, I, S, Br, Rb, aerosol mass concentration, and other elements); (2) a soil dust aerosol component (15.6% of the aerosol mass); (3) a natural biogenic component (18.7% of the aerosol mass and associated with P, K, S, Ca, Sr, Mg, Mn, Cu and Zn); (4) a second soil dust (5.7% of the aerosol mass and enriched in Si, Ti, and Fe); and (5) a NaCl aerosol component (5.9% of the aerosol mass with Na, Cl, Br, and iodine). Electron microscopy analysis of individual aerosol particles confirmed these five aerosol types. Organic material dominated the aerosol mass and the number concentration of airborne particles. Aerosol size distributions show that the fine mode accounts for 78% of the aerosol mass, centered at $0.33 \mu\text{m}$ aerodynamic diameter. The coarse mode accounts for 22% of the mass, centered at about $3.2 \mu\text{m}$. Black carbon size distributions show a consistent picture, with a mass median diameter centered at about $0.175\text{--}0.33 \mu\text{m}$ aerodynamic diameter. This study suggests that for modeling the optical properties of aerosol in the Amazon Basin, it is essential to use a model that includes the optical and physical properties of at least two aerosol components other than the biomass burning aerosol, namely, natural biogenic aerosol and soil dust.

1. Introduction

Rapid deforestation in tropical regions has the potential to change atmospheric composition, as well as climate, over a large portion of the equatorial region [Crutzen and Andreae, 1990; Crutzen and Goldammer, 1993; Gash *et al.*, 1996]. More than 80% of the worldwide emissions from biomass burning originate in the tropics. The high rate of tropical biomass burning in the last decade is mainly a result of burning of savanna in Africa and deforestation in the Amazon Basin [Setzer and Pereira, 1991]. Estimates of total biomass consumed on a global basis range from 2 to 10 Pg (1 petagram = 10^{15} g) per year [Crutzen and Andreae, 1990]. In terms of total particulate matter (TPM), emissions are around 104 Tg (1 tera-

gram = 10^{12} g) per year [Levine, 1990]. For particulate matter in the fine mode (FPM, $d_p < 2.0 \mu\text{m}$), emissions are estimated as 49 Tg yr^{-1} , which accounts for about 7% of the global emissions of fine-mode aerosol. For elemental carbon, the emission of 19 Tg yr^{-1} could account for a high fraction (86%) of the total anthropogenic emissions [Levine, 1990]. These emissions could have regionally significant direct radiative forcing [Hobbs *et al.*, 1997; Holben *et al.*, 1996].

The emissions of gases during biomass burning affect the global concentrations of many gases, including CO, CO₂, CH₄, CH₃Cl, N₂O, COS [Crutzen *et al.*, 1979]. Much less studied are the effects of aerosol emissions. The composition and size distribution of aerosol particles were measured in smoke from forest fires in Rondonia, Brazil where large emissions of potassium, sulfur, silicon, zinc, and organic matter were reported [Artaxo *et al.*, 1993a]. Elemental carbon associated with potassium was identified as a tracer for biomass burning plumes in remote oceanic areas [Andreae, 1983]. The fluxes of trace elements emitted by biomass burning can be significant on a global scale [Echalar *et al.*, 1995]. Many aerosol particles emitted in tropical biomass burning are cloud condensation nuclei (CCN) and can therefore affect the concentrations and sizes of cloud droplets [Hobbs and Radke, 1969; Rogers *et al.*, 1992;

¹Instituto de Física, Universidade de São Paulo, São Paulo, Brazil.

²Department of Atmospheric Sciences, University of Washington, Seattle.

³Institute for Nuclear Sciences, University of Ghent, Ghent, Belgium.

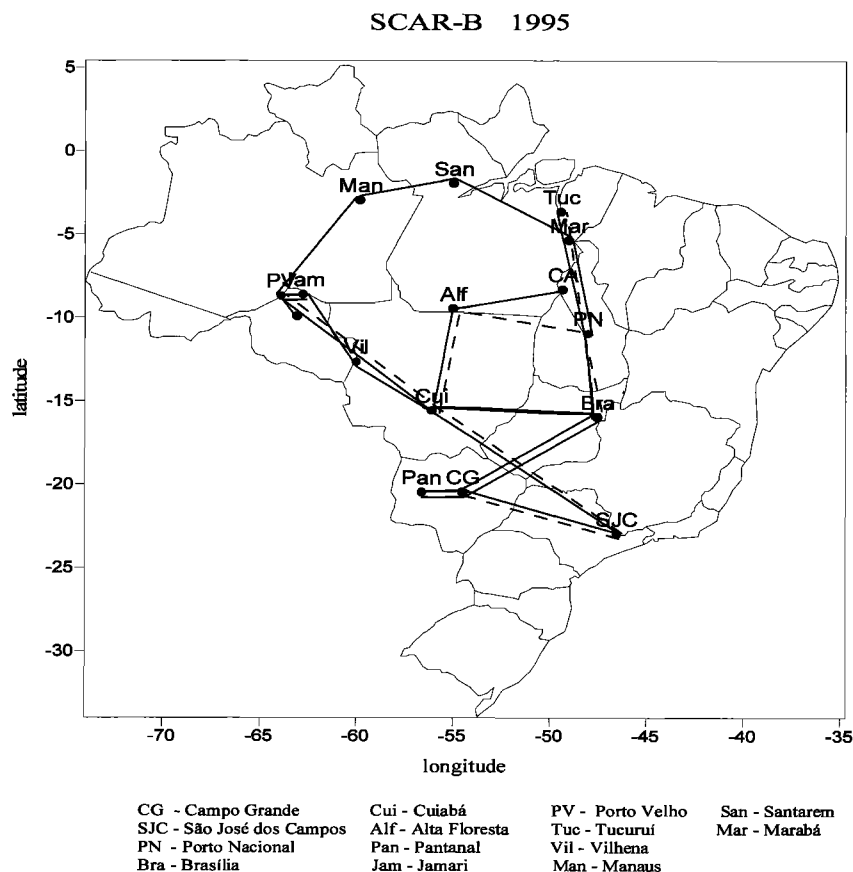


Figure 1. Map of the sampled areas with aircraft flight tracks. Also shown are reference locations codes.

Kaufman and Fraser, 1997]. Therefore the potential exists for changes in precipitation patterns and indirect radiative forcing due to emissions from biomass burning [Kaufman and Tanré, 1994; Kaufman *et al.*, this issue].

Forest vegetation is the principal global source of atmospheric organic particles [Cachier *et al.*, 1985], and in a tropical forest, natural vegetation plays a major role in airborne particle concentrations [Andreae and Crutzen, 1997]. Only a few studies of biogenic aerosols from vegetation in tropical rain forests have been undertaken [Artaxo and Orsini, 1986; Artaxo and Maenhaut, 1990; Artaxo *et al.*, 1988, 1990, 1993b, 1994; Maenhaut *et al.*, 1996a, b]. The natural biogenic aerosols consist of many different types of particles, including pollen, spores, bacteria, algae, protozoa, fungi, fragments of leaves, excrement, and fragments of insects. In addition, a significant fraction of the aerosol is comprised of secondary aerosol, formed by gas-to-particle conversion of organic and sulfur-related biogenic gases. These biogenic particles can be submicrometer in size. Bacteria in forested areas were found in the size range of 0.5 to 2.5 μm [Jaenicke and Mathias-Maser, 1992]. Biological activity of microorganisms on leaf surfaces and forest litter results in airborne particles. Windblown pollens certainly contribute to coarse particles in forested areas. Particulate material containing Zn, Pb, and Cu are produced by higher plants [Beauford *et al.*, 1975, 1977]. The biogenically related elements (e.g., K, P, S, Zn, and Rb) are essential to superior plants. They are present in the fluids circulating in the plant and are released from the leaves to the atmosphere [Nemeruyk, 1970].

The objectives of the present study were to measure aerosol

composition and size distributions over a large area of the Amazon Basin during the biomass burning season and to carry out a quantitative source apportionment study. The use of aircraft for collecting air samples, and the employment of several analytical techniques such as PIXE, INAA, and electron probe X ray microanalysis, allowed a comprehensive study of aerosol characteristics on the large scale in the Amazon Basin.

2. Aerosol Collection and Chemical Analysis

Aerosol particles were collected from three aircraft in various locations in Brazil from August 17 to September 20, 1995, as part of SCAR-B. The flights covered most of the regions of Brazil affected by biomass burning. Two Brazilian Bandeirante EMB 110 aircraft, and the University of Washington Convair C-131A, were used. The Bandeirante is a twin-engine turboprop instrumented aircraft that can fly up to 4–5 km altitude and has a range of about 500 km. Most of the samples were collected aboard the INPE Bandeirante aircraft, but some samples were collected on the FUNCEME (Fundação Cearense de Meteorologia e Recursos Hídricos) Bandeirante aircraft. Isokinetic inlets were installed in ports on both aircraft and were used to collect aerosol particles on Nuclepore and Teflon filters. On the University of Washington's C131A aircraft, aerosol samples were collected continuously from an isokinetic inlet and also from a grab-bag system for aerosols from individual smoke plumes. Typical sampling flow was 10 L min^{-1} for the Nuclepore filter and 18 L min^{-1} for the Teflon samples. The flow rate was measured with precision mass flowmeters. A multi-orifice uniform deposit impactor (MOUDI)

on the C-131A was used to collect size-segregated aerosol samples. The eight-stages of the MOUDI cascade impactor have d_{50} size cuts at 18, 3.2, 1.8, 1.0, 0.56, 0.33, 0.175, and 0.093 μm equivalent aerodynamic diameter. A Teflon after-filter collected all particles smaller than 0.093 μm . The MOUDI has a flow rate of 28 L min^{-1} . The data on the first stage of the MOUDI cascade impactor should be viewed with caution because of possible aircraft nonisokinetic sampling for such large particles. Figure 1 shows the flight tracks that covered most of the areas where biomass burning is a significant source of aerosols during the dry season in the Amazon Basin.

Elemental concentrations on the Nuclepore filters were measured with the particle-induced X ray emission (PIXE) [Johansson and Campbell, 1988] method. It was possible to determine the concentrations of up to 20 elements (Al, Si, P, S, Cl, K, Ca, Ti, V, Cr, Mn, Fe, Ni, Cu, Zn, Br, Rb, Sr, Zr, and Pb). A dedicated 5SDH tandem Pelletron accelerator facility, LAMFI (Laboratório de Análise de Materiais por Feixes Iônicos), from the University of São Paulo was used for the PIXE analysis [Artaxo and Orsini, 1987]. Detection limits are typically 5 ng m^{-3} for elements in the range $13 < Z < 22$ and 0.4 ng m^{-3} for elements with $Z > 23$. The precision of the elemental concentration measurements is typically less than 10%, with 20% for elements with concentration near the detection limit. The aerosol mass concentration was obtained through gravimetric analysis of the Nuclepore and Teflon filters. The filters were weighed before and after sampling in an electronic microbalance with 1 μg sensitivity. Before weighing, the filters were equilibrated for at least 24 hours at 50% relative humidity and 20°C temperature. Electrostatic charges are neutralized by means of ^{210}Po radioactive sources. Detection limit for the aerosol mass concentration is about 0.3 $\mu\text{g m}^{-3}$. Precision is estimated at close to 15%. Black carbon (BC) concentration was measured using a reflectance technique photometer [Andrae, 1983]. A complete description of the method and comparison with other techniques for black carbon determination can be found in the work of Martins *et al.* [this issue]. The INAA analysis procedure is described in detail by Maenhaut *et al.* [1979]. A total of 66 pairs of Nuclepore and Teflon aerosol samples were collected on the three aircraft; and 43 of these were analyzed by PIXE and INAA. Each aerosol sample was collected for a period of 3–4 hours, representing averages of atmospheric concentrations over large areas (100–800 km flight paths).

Individual particle analysis was performed using electron probe X ray microanalysis (EPMA) [Van Grieken *et al.*, 1988, 1991]. The Nuclepore filter loaded with aerosol particles was coated with a thin carbon film and analyzed in a JEOL JSM-T331A scanning electron microscope. The elemental composition was analyzed in a Tracor Noram system, using ZAF correction. A total of 120 particles were analyzed. Cluster analysis of the individual particle data was performed using the IDAS software package [Van Grieken *et al.*, 1988].

3. Absolute Principal Factor Analysis

To separate the different aerosol components, the absolute principal factor analysis (APFA) was used [Thurston and Spengler, 1985; Hopke, 1985]. APFA can provide a quantitative elemental source profile, instead of just a qualitative factor loading matrix as in traditional factor analysis. The absolute elemental source profiles help in the identification of the factors and can be used to quantitatively compare the factor

composition with assumed aerosol sources. The APFA provides the elemental mass contribution of each identified component by calculating the absolute principal factor scores (APFS) for each sample [Artaxo *et al.*, 1988, 1990]. The elemental concentrations are subsequently regressed on the APFS to obtain the contribution of each element for each component. The source profiles thus obtained can be compared with values from the literature to gain information on enrichment and atmospheric chemistry processes [Hopke, 1985]. The measured aerosol mass concentration can be regressed on the APFS to obtain the aerosol total mass source apportionment.

4. Results and Discussions

The aerosol samples represent collection times of 3–4 hours each, and they average atmospheric concentrations over large areas. They do not represent concentrations in individual smoke plumes. Table 1 shows the average, standard deviation, minimum and maximum concentrations of various elements measured in SCAR-B. The sum of the trace elements accounts for 11 to 21% of the aerosol mass. The remaining mass must be organic material, black carbon, water, and other components. The average ratio of black carbon to aerosol mass is 5%, increasing to 8% in areas heavily affected by biomass burning.

For some elements, a wide range of concentrations was observed. Sulphur was observed in concentrations of 59 ng

Table 1. Average, Standard Deviation, Minimum, and Maximum Values of Aerosol Trace Element Concentrations in Airborne Samples During SCAR-B

Element	Mean, ng m^{-3}	Standard Deviation	N^*	Minimum, ng m^{-3}	Maximum, ng m^{-3}
Na	95.4	59.9	43	30.0	270
Mg	659	385	43	196	2356
Al	2292	1808	43	350	7297
Si	3126	2104	43	713	8673
P	140	136	43	3.50	559
S	1198	900	43	59.0	4333
Cl	222	229	43	27.6	1291
K	1581	1076	43	137.3	5581
Ca	1251	1134	43	36.2	5722
Ti	121	123	43	9.29	533
V	3.67	3.43	43	0.54	14.2
Cr	5.14	1.86	18	2.29	8.16
Mn	67.7	64.4	43	10.8	322
Fe	1132	985	43	76.9	4327
Cu	2.90	1.71	43	0.64	8.77
Zn	10.7	6.3	43	1.92	27.7
Rb	8.82	5.32	43	1.55	25.9
Sr	16.4	14.2	43	1.44	59.5
Br	13.1	8.7	43	2.40	36.9
I	3.83	2.11	43	0.64	9.18
Ga	0.49	0.34	43	0.01	1.46
La	0.78	0.61	43	0.19	2.97
Sm	0.11	0.092	43	0.003	0.42
Th	0.36	0.23	43	0.045	1.17
Sc	0.36	0.35	43	0.041	1.47
As	0.21	0.16	31	0.041	0.85
Sb	0.12	0.06	27	0.025	0.27
Zr	6.10	3.69	24	2.08	15.7
Mass†	107	61	43	8.05	297
BC†	5.49	3.92	43	0.23	17.5

* N is the number of samples where the element was observed above its detection limit.

†Aerosol mass and black carbon (BC) are expressed in $\mu\text{g m}^{-3}$.

Aerosol Mass Concentration - SCAR-B

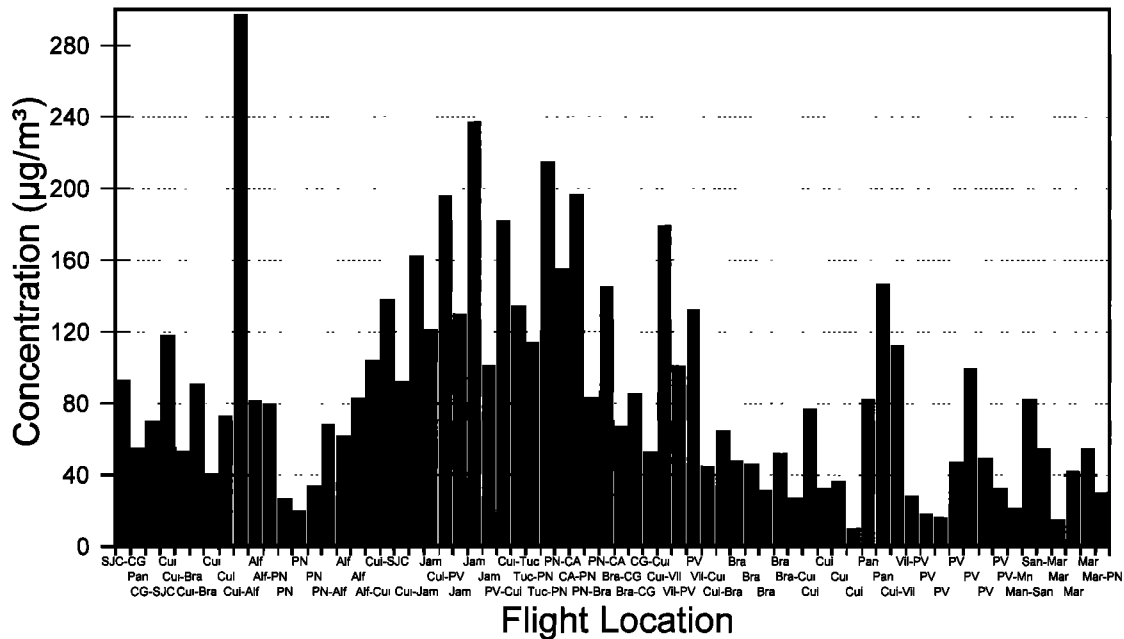


Figure 2. Aerosol mass concentrations observed in each location at the SCAR-B experiment. Maximum concentrations were observed in Rondonia and Alta Floresta regions.

m^{-3} in areas not severely affected by biomass burning and $4330 \text{ ng } m^{-3}$ in areas with heavy smoke. Average aerosol mass concentrations up to $297 \text{ } \mu\text{g } m^{-3}$ were observed; in areas not heavily affected by biomass burning, the average aerosol mass concentration was about $10\text{--}20 \text{ } \mu\text{g } m^{-3}$. The latter range of values is compatible with aerosol mass concentrations measured in the wet season in Brazil, when no biomass burning occurs [Artaxo et al., 1994, 1997]. The elemental compositions

observed are compatible with ground-based measurements in Cuiabá during the dry season [Maenhaut et al., 1996a]. Very high black carbon concentrations up to $17.5 \text{ } \mu\text{g } m^{-3}$ were observed; these values are consistent with the absorption measurements in SCAR-B [Martins et al., this issue; Reid et al., this issue].

Figure 2 shows the individual aerosol mass concentrations observed in SCAR-B. Higher concentrations were observed in

Black Carbon Concentration - SCAR-B

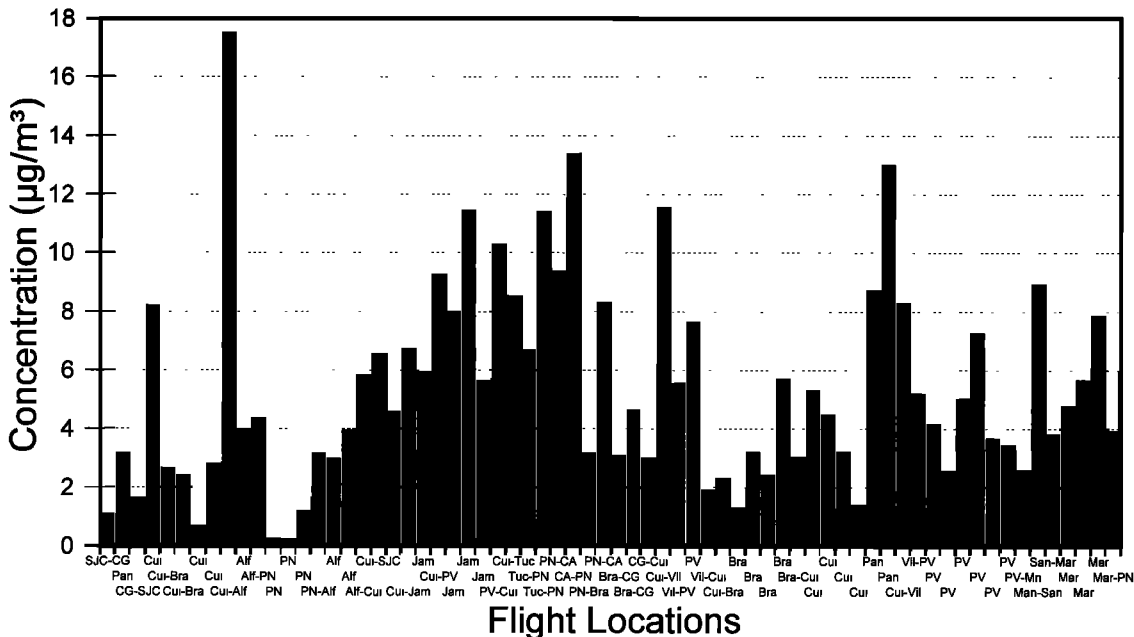


Figure 3. Black carbon concentration observed in each location at the SCAR-B experiment.

Table 2. VARIMAX-Rotated Factor Loading Matrix for Aircraft Aerosol Samples Collected in SCAR-B Experiment

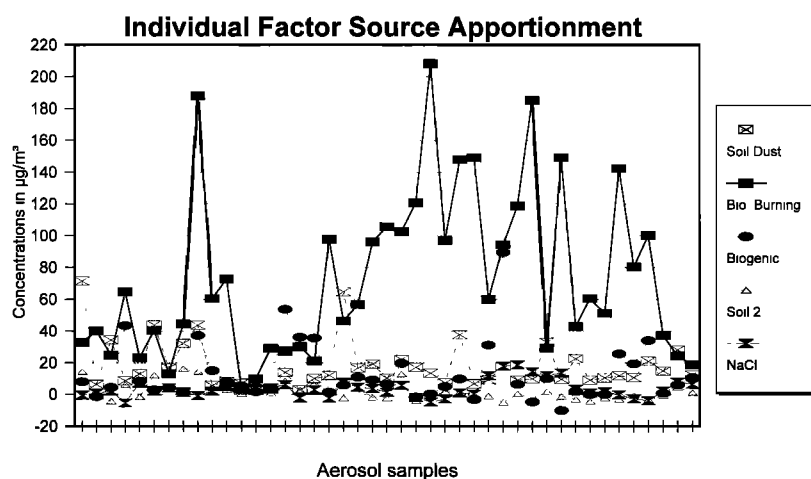
	Factor 1 Soil Dust	Factor 2 Biomass Burning	Factor 3 Natural Biogenic	Factor 4 Soil 2	Factor 5 NaCl	Communi- alities
Sm	0.97	-0.01	0.06	-0.02	0.09	0.95
Sc	0.97	-0.04	-0.03	0.13	-0.02	0.96
Al	0.96	0.07	0.00	0.20	-0.02	0.97
La	0.95	0.03	0.15	-0.09	0.08	0.94
Th	0.94	0.10	0.01	0.08	-0.11	0.91
V	0.92	-0.05	-0.01	0.13	-0.02	0.87
Ga	0.87	0.22	0.17	0.08	0.25	0.90
Ti	0.74	0.12	0.08	0.63	0.00	0.97
Fe	0.72	0.14	0.01	0.64	-0.02	0.96
BC	0.08	0.91	0.30	0.09	0.10	0.94
S	-0.03	0.90	0.28	0.19	0.01	0.93
I	-0.02	0.87	0.29	0.06	0.32	0.95
Mass	0.28	0.86	0.23	0.05	0.16	0.90
Zn	0.13	0.78	0.51	0.19	0.04	0.92
Br	-0.15	0.75	0.46	-0.09	0.31	0.90
K	-0.03	0.72	0.62	-0.04	0.16	0.93
Rb	0.21	0.67	0.39	0.45	-0.24	0.91
Ca	-0.03	0.30	0.91	0.05	0.02	0.92
Sr	-0.05	0.27	0.87	0.10	-0.16	0.87
P	0.02	0.35	0.86	0.21	-0.00	0.91
Mg	0.25	0.27	0.83	-0.11	0.24	0.89
Mn	0.14	0.35	0.82	0.16	0.13	0.86
Cl	0.01	0.50	0.66	0.01	0.42	0.86
Cu	0.26	0.39	0.59	0.47	-0.07	0.79
Si	0.38	0.31	0.48	0.61	0.25	0.91
Na	0.09	0.37	0.08	0.03	0.86	0.89
Var.	7.7	6.5	6.1	1.9	1.5	

the Rondonia and Alta Floresta areas, where intense deforestation is going on. Low values in Figure 2 of about $10\text{--}20\ \mu\text{g m}^{-3}$ are representative of regions with little impact of smoke, affected mostly by natural biogenic aerosol particles emitted by the forest.

The black carbon concentration for each airborne sample is shown in Figure 3. BC values varied from a low $0.20\ \mu\text{g m}^{-3}$ in areas not heavily affected by biomass burning to values up to $17\ \mu\text{g m}^{-3}$ in areas heavily affected by smoke. *Robock* [1988] has documented noticeable surface cooling with the presence of even lower levels of forest fire smoke. In general, BC represents 5–10% of the aerosol mass concentration, depending

on the impact of the different aerosol sources, and the age of the smoke [*Martins et al.*, this issue; *Reid et al.*, this issue].

The variability in the concentrations of trace elements, together with the mass and the BC concentrations, were used in a factor analysis model to study the relationship between the observed variables. Table 2 shows the VARIMAX-rotated factor loading matrix. Column 7 in Table 2 shows the communalities of the factor analysis that expresses the percentage of each element variability that was explained by the factor model. The last line in Table 2 gives the variance explained by each retained factor. The first factor has high loadings for Al, Sm, Sc, La, Th, V, Ga, Ti, and Fe and represents soil and dust aerosol particles. The second component is associated with the biomass burning aerosol, with high loadings for BC, S, I, Br, Zn, K, Rb, Cl, and aerosol mass, mainly representing the high organic aerosol component. The third component is loaded with Ca, Sr, P, Mg, K, Mn, Cl, Zn, and Cu. The low black carbon loading, and the presence of phosphorus, indicates that this component represents natural biogenic aerosol particles. Factor 4 is associated with Si, Fe, and Ti, representing a second component of soil dust particles. The last factor has associations with Na and Cl and somewhat with bromine and iodine, indicating that it could be associated with marine aerosol particles. As the Amazon Basin region is composed of several different types of soils, and the area covered by the flights was very large, it is not surprising to find two different soil dust components. Also, the second soil dust component could be associated with a combination of soil resuspension, together with forest litter and ash, causing the separation of soil dust in two different components. As for the NaCl aerosol component, intrusions of Atlantic marine air masses are common in the Amazon Basin. A marine aerosol component was already observed in the Amazon Basin, as described previously by *Artaxo et al.* [1988] and *Talbot et al.* [1990]. The meteorological conditions associated with this transport were characterized by *Garstang et al.* [1990] and by *Greco et al.* [1990]. However, taking in account that this component was also sometimes observed in Rondonia, at 3000 km from the Atlantic Ocean, it is not possible to rule out a local source for the NaCl. *Reid et al.* [this issue] also observed a similar NaCl component in aerosol samples collected at the C-131A aircraft at the SCAR-B experiment. The factor analysis results reported here

**Figure 4.** Absolute aerosol source apportionment for each component and each sample.

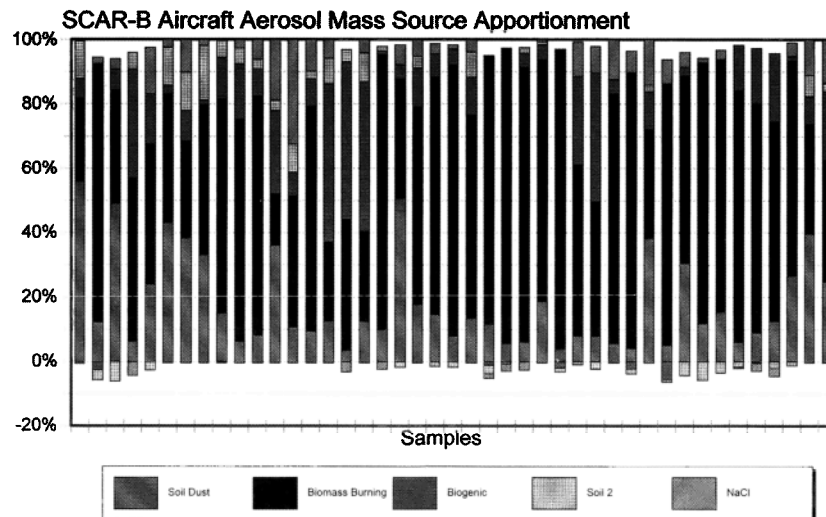


Figure 5. Aerosol source apportionment in terms of percentage of the observed aerosol mass for each sample and each component.

are similar to other ground-based aerosol source apportionment studies in the Amazon Basin [Artaxo *et al.*, 1995, 1997; Maenhaut *et al.*, 1996b, Echalar *et al.*, this issue]. Similar characteristic elements for biomass burning emissions have been associated with biomass burning aerosol in Africa [Lacaux *et al.*, 1993; Gaudichet *et al.*, 1995]. The five component model explains 91% of the data variance, and the first three components account for 78%. The communalities for all variables are, in general, larger than 90%, meaning that the five factors could explain satisfactorily the observed elemental concentrations.

It is surprising to observe a natural biogenic aerosol component in the dry season with such high aerosol loading from biomass burning. The aerosol mass concentration in the Amazon Basin during the wet season (with no biomass burning) range from 10 to 15 $\mu\text{g m}^{-3}$ for particles less than 10 μm [Echalar *et al.*, this issue]. This is a considerable aerosol mass concentration. In the fine mode ($d_p < 2 \mu\text{m}$) the aerosol mass concentration is a significant 2–5 $\mu\text{g m}^{-3}$. There are two main sources for these natural biogenic particles: primary biogenic aerosol particles, rich in organic matter plus P, K, S, Ca, Mn, Zn, Cl, and other elements, and the gas-to-particle conversion from biogenic VOCs. This aerosol component is part of the natural biosphere-atmosphere exchange and is a component of the vegetation metabolism (through the nutrient cycling). This natural component is present all the time in the Amazon, during the dry and wet season. However, in the dry season the aerosol mass concentration is dominated by biomass burning aerosol particles, although the natural biogenic component is always present. The nature and mechanism of emission for part of these particles is unknown.

The quantitative aerosol source apportionment for each observed component and each aerosol sample is shown in Figure 4. The results are indicated as mass concentrations (in $\mu\text{g m}^{-3}$) for each of the five components for each sample. The impacts of biomass burning, soil dust, and biogenic components are of the same order of magnitude for the first seven samples. From the middle of SCAR-B on, biomass burning dominated significantly the atmospheric aerosol loading. The masses associated with the NaCl aerosol and the soil 2 component were very

small during this period. The soil dust component was always present in significant amounts, of the order of 10–40 $\mu\text{g m}^{-3}$. August and September represents the peak of the dry season, with significant fraction of bare soil exposed in the cerrado areas of central Brazil.

The aerosol source apportionment in terms of percentage of the observed aerosol mass for each sample and each component can be observed in Figure 5. For some samples, the biomass burning aerosol accounted for 70–90% of the aerosol mass, but it is noteworthy that for most of the samples, there were significant amounts of soil dust and natural biogenic aerosol. The small negative values in the aerosol source apportionment are always below 7%. Given that the combined analytical uncertainty is around 10% for most of the elements, these small negative values are within the measurement standard deviation. Biogenic aerosol is the most important component for four of the samples, while soil dust is the most important component for five samples. This implies that in order to model the optical properties of aerosol in the Amazon Basin it is essential to include the optical and physical properties of natural biogenic aerosol and soil dust, in addition to

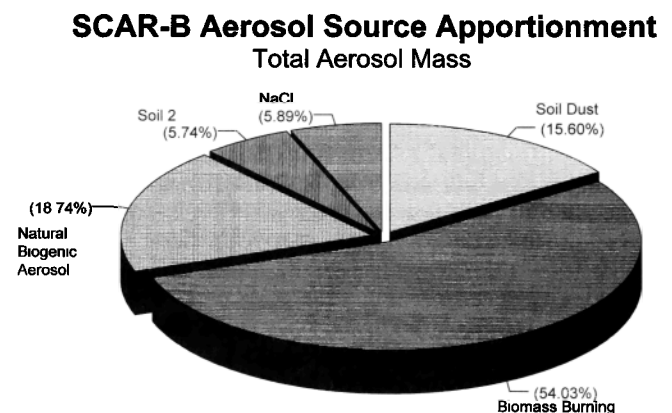


Figure 6. Total aerosol mass source apportionment for the SCAR-B aircraft aerosol samples in Brazil.

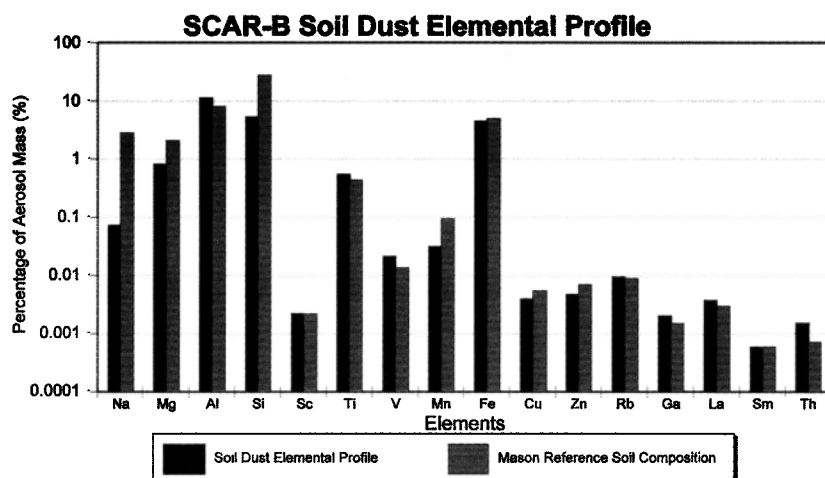


Figure 7. Elemental compositions of the soil dust component measured in SCAR-B. Also shown is the average crustal abundance given by *Mason* [1966].

biomass burning smoke. This is achieved by measuring the properties of regional hazes dominated by smoke from biomass burning.

Figure 6 shows the total aerosol mass source apportionment. For the SCAR-B aircraft samples, 54.0% of the aerosol mass was associated with biomass burning aerosol, 18.7% with natural biogenic aerosol, 15.6% with soil dust, 5.7% with a second soil dust component, and 5.9% with the NaCl aerosol. These values represent the average for all samples collected in SCAR-B.

Using the APFA technique, it is possible to derive absolute elemental profiles for each of the components. Figure 7 shows the elemental source profile for the soil dust component. A comparison with the average crustal abundance given by *Mason* [1966] is included. The elemental profile from the APFA procedure shows a very similar elemental pattern to that of average crustal material. The main discrepancies are for silicon and sodium. It is important to note, however, that there is a second soil dust component discriminated by the APFA model that has silicon as its main element. The elemental source

profile for the biomass burning component is shown in Figure 8. The observed elemental profile was compared with particles collected directly over fires in the cerrado and forest regions of Brazil [*Yamasoe*, 1995]. Potassium was measured in SCAR-B as 1.46% of the aerosol mass, while in direct emissions by *Yamasoe* [1995], it was observed at 1.38%. Black carbon was measured in SCAR-B at 6.3% of the aerosol mass, while in direct emissions, it was measured at 7.6%. Chlorine in SCAR-B was observed at much lower concentrations, due to the volatilization in the atmosphere after the emissions from the fires. Sulphur was observed at higher values than in the direct emissions, probably due to assimilation and incorporation of gaseous sulphur compounds in existing aerosol particles after the emissions. Zinc was observed in similar concentrations, and it was measured in SCAR-B a factor of 2 higher phosphorus concentrations than in the work of *Yamasoe* [1995]. The direct emission measurements by *Yamasoe* [1995] were performed at a few meters away from the fires, so freshly emitted aerosol particles were collected, while the aircraft measurements reported here represent a regional average of

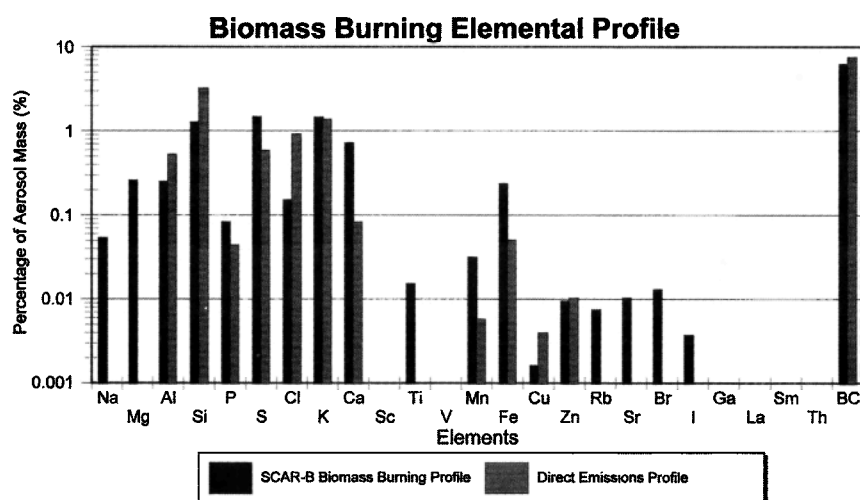


Figure 8. Elemental source profile for the biomass burning component measured in SCAR-B compared with measurements obtained directly over the fires in the forested and cerrado regions of Brazil [*Yamasoe*, 1995].

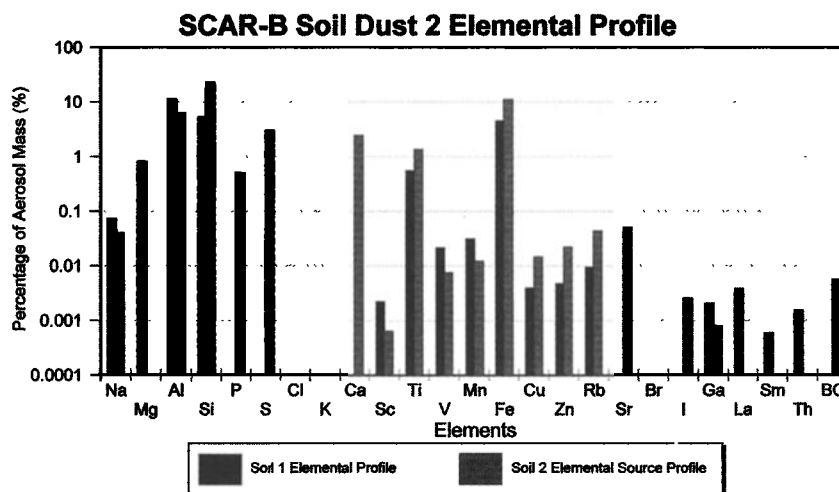


Figure 9. Comparison of the elemental profile for the two soil dust components in SCAR-B.

aged aerosol. Reid *et al.* [this issue] and Reid and Hobbs [this issue] discuss mechanisms for the very rapid evolution of young smoke particles, which can explain the differences in the elemental profiles shown in Figure 8.

Figure 9 compares the elemental profiles for the two soil dust components observed in this study. The second soil dust factor (soil 2) shows higher Si, Ti, and Fe concentrations, as well as the presence of calcium, which was absent in the first soil dust component. In addition, S and P are present in significant amounts, indicating the presence of some biological material in this component. In view of the presence of biogenically related elements, this aerosol component could represent resuspended forest litter. Enrichments of Zn, Rb, Sr, and iodine support this view. The high amount of BC in this component may be associated with resuspension of ash particles deposited on the soil, which may have a significant effect on light absorption. Also, strong atmospheric convection in burning areas could simultaneously loft both soil dust and biomass burning particles into the atmosphere.

The aerosol size distribution was measured with the MOUDI cascade impactor. A total of seven size distribution measurements were made on the C-131A aircraft. The aerosol mass distributions obtained are shown in Figure 10. The mass concentration indicated in the first MOUDI stage should be

viewed with caution because of possible nonisokinetic aircraft sampling for this size range. The peak of the size distribution is at $0.33 \mu\text{m}$ diameter for most of the samples. A small coarse mode component is centered at about $3.2 \mu\text{m}$ diameter. For these seven cascade impactor samples collected over different regions, the average fine mode mass ($d_p < 1 \mu\text{m}$) accounts for 78%, while the coarse mode mass ($d_p > 1 \mu\text{m}$) is 22% of the total mass. These fractions are characteristic of aerosols collected from aircraft in the regional hazes in the Amazon Basin [Pereira *et al.*, 1996]. Also, the average diameter observed is consistent with those of aged natural biogenic aerosol particles measured on the ground [Artaxo and Hanson, 1990].

With the aerosol samples collected with the rotating version of the MOUDI cascade impactor, it is possible to perform a reflectance measurement of the aerosol deposit and obtain black carbon concentrations [Andreae, 1983; Andreae *et al.*, 1984]. Figure 11 shows the black carbon aerosol size distribution for each of the collected MOUDI cascade impactors. The average aerodynamic diameter is between 0.175 and $0.33 \mu\text{m}$. Very little or no black carbon was observed above $1 \mu\text{m}$ diameter.

Some selected samples were subjected to individual particle analysis by EPMA. This analysis allows the study of particle morphology and composition. The EPMA was performed only on particles larger than $0.3 \mu\text{m}$ diameter, due to the resolution

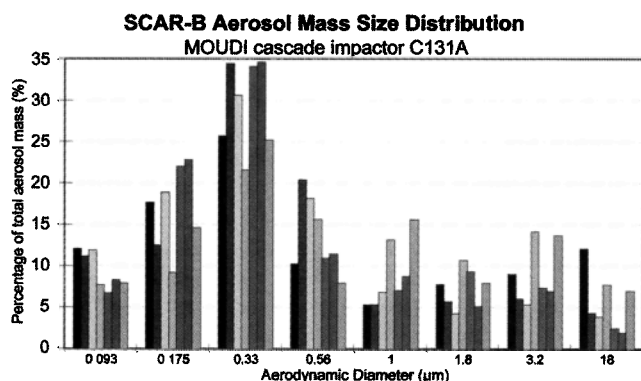


Figure 10. Aerosol mass size distribution for the seven MOUDI cascade impactor samples collected aboard the C-131A aircraft in SCAR-B.

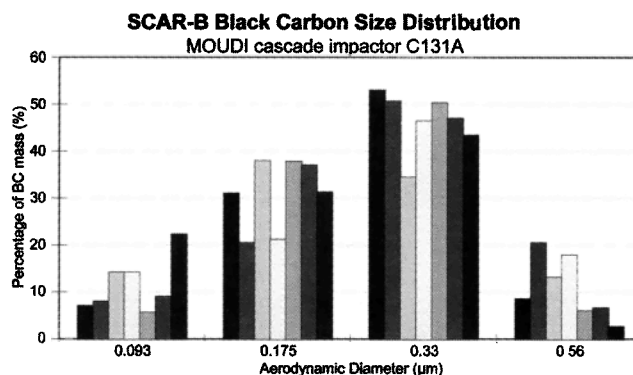


Figure 11. Black carbon size distribution for the seven MOUDI cascade impactor samples collected aboard the C-131A aircraft in SCAR-B.

SCAR-B Individual particle analysis

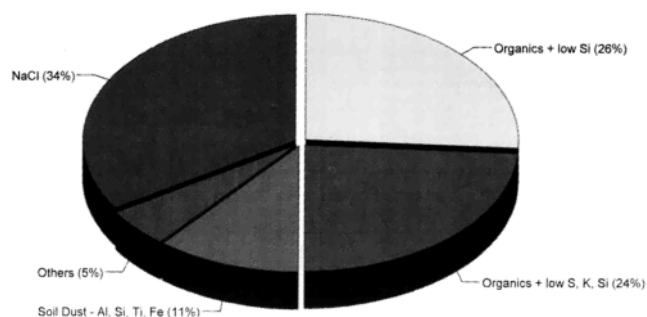


Figure 12. Individual particle analysis by electron probe X ray microanalysis of two aerosol samples collected aboard the C-131A in Jamari, Rondonia, at altitudes from 600 to 4000 m in SCAR-B.

of the instrument and the carbon coating of the particles, that is needed for X ray microanalysis. Figure 12 shows the cluster analysis of two aerosol samples collected near Jamari, Rondonia, at altitudes from 600 to 4000 m. Half of the measured particles were primarily organic, but with small amounts (of the order of 0.5 to 1% in mass) of silicon, sulphur, and potassium. This large organic group represents biomass burning and natural biogenic particles. The elements that could be used for

distinguishing between the two particle groups could not be observed within the detection limit of the EPMA analysis (about 0.5% in mass). These two subgroups of organic particles had average diameters of $1.3 \pm 1.0 \mu\text{m}$ and $0.9 \pm 0.6 \mu\text{m}$, respectively. The group of particles containing NaCl comprised 34% of the measured particles and corresponded to larger particles (average diameter $2.2 \pm 2.6 \mu\text{m}$). This is a surprisingly high abundance, taking into account that the measurements were made 3000 km from the Atlantic Ocean. Talbot *et al.* [1990] and Swap *et al.* [1996] observed strong effects of long-range transport in the Amazon Basin. Aerosol samples collected over the same region in this work show up to 7000 ng m^{-3} for chlorine and 135 ng m^{-3} for bromine. It is not possible unequivocally to conclude whether the NaCl particle class represents marine aerosol particles or instead consists of soil particles rich in NaCl. The soil dust particle accounts for 11% of the number concentration of particles, a value consistent with the APFA results, with a mean diameter of $1.9 \pm 0.8 \mu\text{m}$. A small amount (5%) of the particles, with a mean diameter of $0.7 \pm 0.3 \mu\text{m}$ are mixed groups. This could be the result of processing through clouds, or these particles could represent an internal mixture of different particle types. It is important to emphasize that the EPMA accounts only for particles larger than $0.3 \mu\text{m}$ in diameter, which account for most of the aerosol mass. However, in terms of the number of particles, the majority is below $0.3 \mu\text{m}$ diameter.

One of the important aspects of analyzing aerosols in large

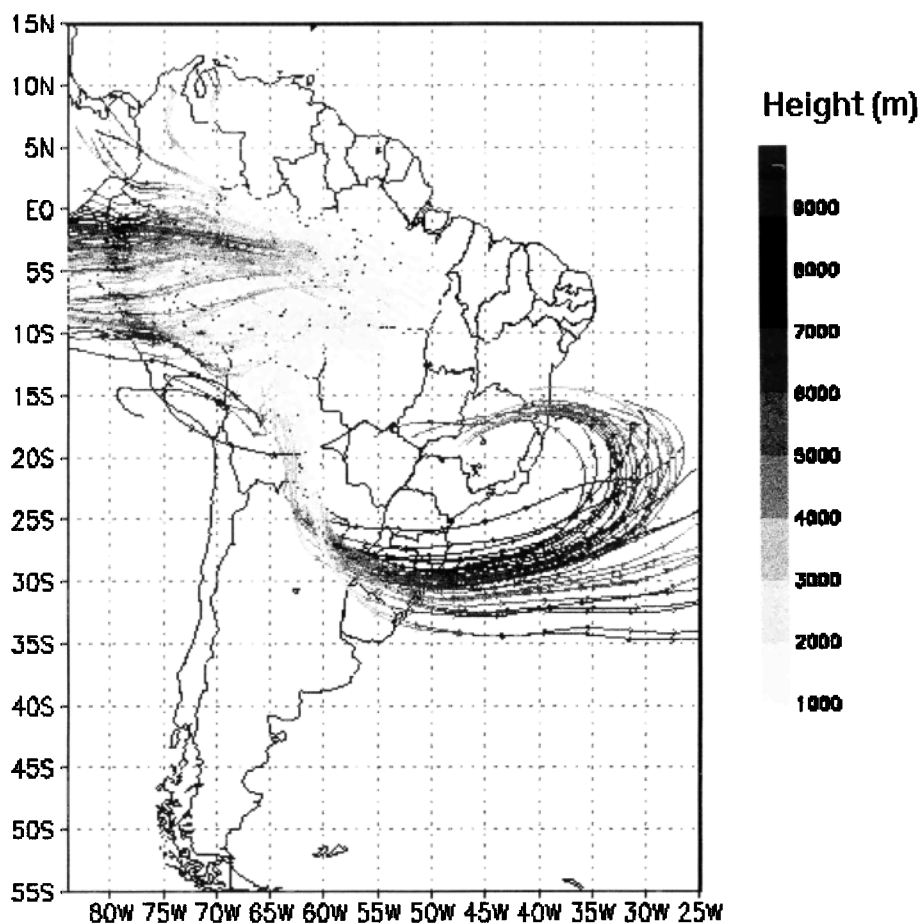


Figure 13. Three-dimensional forward air mass trajectories starting in biomass burning spots on August 22, 1985, during the SCAR-B experiment.

scale is the issue of long-range transport. Three-dimensional (3-D) air mass trajectories were calculated starting from biomass burning spots provided by A. Setzer (INPE) for the latest part of August 1995, during the SCAR-B experiment [Setzer *et al.*, 1994]. Complete details of results and model used can be obtained in the work by Freitas *et al.* [1997]. The 3-D trajectories were determined from the wind fields generated by the Regional Atmospheric Modeling System (RAMS) model described by Pielke *et al.* [1992]. The model is nudged at every time step toward a global analysis available every 12 hours. The model vertical resolution starts at 100 m in lower levels stretching at a rate of 1.2 up to 1200 m and then keeping a constant resolution up to model top located at 15.5 km. It was observed that one approaching cold front in the last week of September 1995 provides a conveyor belt where sloping ascent of the 3-D trajectories takes place. This movement transports gases and aerosol particles up to the upper troposphere. Figure 13 shows the 3-D forward air mass trajectories starting in biomass burning spots on August 22, 1985, during the SCAR-B experiment. It is possible to observe that after 7–8 days the air masses have two preferential flows: along the Andes and in the South Atlantic. The corresponding GOES visible image shows a similar aerosol pattern than the 3-D trajectory model. The TOMS aerosol product also shows higher aerosol concentrations along the southern part of the Atlantic Ocean and in the Pacific, with a similar transport pattern than the one presented in Figure 13. This long-range pattern was observed frequently during the SCAR-B experiment. This long-range transport of gases and aerosol particles may have a significant climate impact in the southern hemisphere as well as important regional impacts in the South American continent.

5. Conclusions

The large-scale picture of aerosols in the Amazon Basin during the biomass burning season described in this paper reveals a variety of particle types. A large variability in the amount of the aerosol particles was observed from site to site. Biomass burning aerosols dominated the aerosol mass in most cases. Surprisingly, natural biogenic aerosol particles show a consistent presence, and for sites with low loading of smoke, the natural biogenic component dominates. Soil dust particles also show a consistent presence, probably due to the dryness of the soil and strong convective movements. A small NaCl component was observed (about 5.9% of the aerosol mass). The origin of this component is unclear; local sources or long-range transport of marine aerosol are both possibilities. Organic material dominated the aerosol mass and the number of particles. Aerosol size distributions showed that the fine mode accounts for 78% of the aerosol mass, centered at $0.33 \mu\text{m}$ aerodynamic diameter. The coarse mode accounts for 22% of the mass, centered at about $3.2 \mu\text{m}$. Black carbon size distribution exhibited a consistent picture, with mass median diameter centered at about $0.175\text{--}0.33 \mu\text{m}$ aerodynamic diameter. Three-dimensional air mass trajectories and satellite images show two main paths, along the Andes and to the South Atlantic Ocean. Significant fluxes of aerosol particles enter the southern atmosphere through these two pathways, at high altitudes.

The results from this work suggest that for modeling the optical properties of aerosol in the Amazon Basin, it is essential to work with an aerosol model that includes optical properties for at least three aerosol components, namely, natural

biogenic aerosol and soil dust, in addition to the biomass burning aerosol.

Acknowledgments. Thanks are due to Ronald Ferek and Jeffrey Reid for help during the C-131A sampling. We thank Alcides C. Ribeiro, Ana L. Loureiro, Manfredo Tabacniks, and Tarsis Germano for assistance during sampling and PIXE analysis. We also thank Volker Kirchhoff, Yoram Kaufman, Dave Mc Dougal, and the SCAR-B team for help in planning and data interpretation. This work was financed through grants 90/2950-2, 96/2672-9, 96/2671-2, 97/00844-0 from FAPESP-Fundação de Amparo à Pesquisa do Estado de São Paulo. The University of Washington's participation was supported by grants NASA NAGW-3750 and NAG 11709; NSF ATM-9400760, ATM-9412082, and ATM-9408941; NOAA NA37RJ 0198AM09; and EPA CR822077. One of us (W.M.) acknowledges the financial support from the Belgian State, Prime Minister's Service, Federal Office for Scientific, Technical, and Cultural Affairs (OSTC) and from the Fonds voor Wetenschappelijk Onderzoek, Vlaanderen.

References

- Andreae, M. O., Soot carbon and excess fine potassium: Long-range transport of combustion derived aerosols, *Science*, 220, 1148–1151, 1983.
- Andreae, M. O., and P. J. Crutzen, Atmospheric aerosols: Biogeochemical sources and role in atmospheric chemistry, *Science*, 276, 1052–1058, 1997.
- Andreae, M. O., et al., Biomass burning emissions and associated haze layers over Amazonia, *J. Geophys. Res.*, 93, 1509–1527, 1984.
- Artaxo, P., and H. C. Hansson, Size distribution and trace element concentration of atmospheric aerosols from the Amazon Basin, in *Aerosols: Science, Industry, Health and Environment*, edited by S. Masuda and K. Takahashi, pp. 1042–1045, Elsevier, New York, 1990.
- Artaxo, P., and H.-C. Hansson, Size distribution of biogenic aerosol particles from the Amazon Basin, *Atmos. Environ.*, 29(3), 393–402, 1995.
- Artaxo, P., and W. Maenhaut, Trace element concentrations and size distribution of biogenic aerosols from the Amazon Basin during the wet season, *Nucl. Instrum. Methods Phys. Res., Sec. B*, 49, 366–371, 1990.
- Artaxo, P., and C. Orsini, The emission of aerosol by plants revealed by three receptor models, in *Aerosols: Formation and Reactivity*, edited by G. Israel, pp. 148–151, Pergamon, New York, 1986.
- Artaxo, P., and C. Orsini, PIXE and receptor models applied to remote aerosol source apportionment in Brazil, *Nucl. Instrum. Methods Phys. Res., Sec. B*, 22, 259–263, 1987.
- Artaxo, P., H. Storms, F. Bruynseels, R. Van Grieken, and W. Maenhaut, Composition and sources of aerosols from the Amazon Basin, *J. Geophys. Res.*, 93, 1605–1615, 1988.
- Artaxo, P., W. Maenhaut, H. Storms, and R. Van Grieken, Aerosol characteristics and sources for the Amazon Basin during the wet season, *J. Geophys. Res.*, 95, 16,971–16,985, 1990.
- Artaxo, P., M. Yamasoe, J. V. Martins, S. Kocinas, S. Carvalho, and W. Maenhaut, Case study of atmospheric measurements in Brazil: Aerosol emissions from Amazon Basin biomass burning, in *Fire in the Environment: The Ecological, Atmospheric, and Climatic Importance of Vegetation Fires*, edited by P. J. Crutzen and J.-G. Goldammer, pp. 139–158, John Wiley, New York, 1993a.
- Artaxo, P., F. Gerab, and M. L. C. Rabello, Elemental composition of aerosol particles from two background monitoring stations in the Amazon Basin, *Nucl. Instrum. Methods Phys. Res., Sec. B*, 75, 277–281, 1993b.
- Artaxo, P., F. Gerab, M. A. Yamasoe, and J. V. Martins, Fine mode aerosol composition in three long-term atmospheric monitoring sampling stations in the Amazon Basin, *J. Geophys. Res.*, 99, 22,857–22,868, 1994.
- Artaxo, P., F. Gerab, M. A. Yamasoe, and J. V. Martins, The chemistry of atmospheric aerosol particles in the Amazon Basin, in *Chemistry of the Amazon: Biodiversity, Natural Products and Environmental Concerns*, *Am. Chem. Soc. Book Ser., ACS Symp. Ser. 588*, edited by P. R. Seidl, O. R. Gottlieb, and M. A. C. Kaplan, pp. 265–280, Washington, D. C., 1995.
- Artaxo, P., F. Gerab, and M. A. Yamasoe, Long term atmospheric aerosol characterization in the Amazon Basin, in *Environmental Geochemistry in the Tropics*, edited by J. Wasserman, E. V. Silva Filho, and R. Villas Boas, pp. 227–250, Springer-Verlag, New York, 1997.

- Beauford, W., J. Barber, and A. R. Barringer, Heavy metal release from plants into the atmosphere, *Nature*, 256, 35–37, 1975.
- Beauford, W., J. Barber, and A. R. Barringer, Release of particles containing metals from vegetation into the atmosphere, *Science*, 195, 571–573, 1977.
- Cachier, H., P. Buat-Ménard, M. Fontugne, and J. Rancher, Source terms and source strengths of the carbonaceous aerosol in the tropics, *J. Atmos. Chem.*, 3, 469–489, 1985.
- Crutzen, P., and M. O. Andreae, Biomass burning in the tropics: Impact on atmospheric chemistry and biogeochemical cycles, *Science*, 250, 1669–1678, 1990.
- Crutzen, P. J., and J. G. Goldammer, (Eds.), *Fire in the Environment: The Ecological, Atmospheric and Climatic Importance of Vegetation Fires*, John Wiley, New York, 1993.
- Crutzen, P. J., L. E. Heidt, J. P. Krasnec, W. H. Pollock, and W. Seiler, Biomass burning as a source of the atmospheric gases CO, H₂, N₂O, NO, CH₃Cl and COS, *Nature*, 282, 253–256, 1979.
- Echalar, F., A. Gaudichet, H. Cachier, and P. Artaxo, Aerosol emissions by tropical forest and savanna biomass burning: Characteristic trace elements and fluxes, *Geophys. Res. Lett.*, 22, 3039–3042, 1995.
- Freitas, S. R., K. M. Longo, M. A. F. Silva Dias, and P. Artaxo, Numerical modelling of air mass trajectories from the biomass burning areas of the Amazon Basin, *Ann. Acad. Bras. Cienc.*, 68, 193–206, 1997.
- Garstang, M., R. Swap, S. Greco, R. Harriss, R. Talbot, M. Shipham, V. Connors, and P. Artaxo, The Amazon Boundary Layer Experiment: A meteorological perspective, *Bull. Am. Meteorol. Soc.*, 71, 19–32, 1990.
- Gash, J. H. C., C. A. Nobre, J. M. Hoberts, and R. L. Victoria, Amazon deforestation and climate, John Wiley, New York, 1996.
- Gaudichet, A., F. Echalar, B. Chatenet, J. P. Quisefit, G. Malingre, H. Cachier, P. Buat-Ménard, P. Artaxo, and W. Maenhaut, Trace elements in tropical African savanna biomass burning aerosols, *J. Atmos. Chem.*, 22, 19–39, 1995.
- Greco, S., R. Swap, M. Garstang, S. Ulanski, M. Shipham, R. C. Harriss, R. Talbot, M. O. Andreae, and P. Artaxo, Rainfall and surface kinematic conditions over central Amazonia during ABLE 2B, *J. Geophys. Res.*, 95, 17,001–17,014, 1990.
- Hobbs, P. V., and L. F. Radke, Cloud condensation nuclei from a simulated forest fire, *Science*, 163, 279–280, 1969.
- Hobbs, P. V., J. S. Reid, R. A. Kotchenruther, R. J. Ferek, and R. Weiss, Direct radiative forcing by smoke from biomass burning, *Science*, 275, 1776–1778, 1997.
- Holben, B. N., T. F. Eck, A. Pereira, and I. Slutsker, Effect of dry season biomass burning on Amazon Basin aerosol concentrations and optical properties, 1992–1994, *J. Geophys. Res.*, 101, 19,455–19,464, 1996.
- Hopke, P. K., *Receptor Modeling in Environmental Chemistry*, John Wiley, New York, 1985.
- Jaenicke, R., and S. Mathias-Maser, Natural sources of atmospheric aerosol particles, in *Precipitation Scavenging and Atmosphere-Surface Exchange*, edited by S. E. Schwartz and W. G. N. Slinn, pp. 1617–1639, Hemisphere, Bristol, Pa., 1992.
- Johansson, S. A. E., and J. L. Campbell, *PIXE—A Novel Technique for Elemental Analysis*, John Wiley, New York, 1988.
- Kaufman, Y. J., and R. S. Fraser, The effect of smoke particles on clouds and climate forcing, *Science*, 277, 1636–1639, 1997.
- Kaufman, Y. J., and D. Tanré, Variations in cloud supersaturation and the aerosol indirect effect on climate, *Nature*, 369, 45–48, 1994.
- Kaufman, Y. J., et al., Smoke, Clouds, and Radiation—Brazil (SCAR-B) experiment, *J. Geophys. Res.*, this issue.
- Lacaux, J.-P., H. Cachier, and R. Delmas, Biomass burning in Africa: An overview of its impact on atmospheric chemistry, in *Fire in the Environment: The Ecological, Atmospheric, and Climatic Importance of Vegetation Fires*, edited by P. J. Crutzen and J.-G. Goldammer, pp. 159–191, John Wiley, New York, 1993.
- Levine, J., Global biomass burning: Atmospheric, climatic and biospheric implications, *Eos Trans. AGU*, 71(37), 1075–1077, 1990.
- Maenhaut, W., W. H. Zoller, R. A. Duce, and G. L. Hoffman, Concentrations and size distributions of particulate trace elements in the south polar atmosphere, *J. Geophys. Res.*, 84, 2421–2431, 1979.
- Maenhaut, W., G. Koppen, and P. Artaxo, Long term atmospheric aerosol study in Cuiabá, Brazil: Multielemental composition, sources, and impacts of biomass burning, in *Biomass Burning and Global Change*, edited by Joel Levine, pp. 637–652, MIT Press, Cambridge, Mass., 1996a.
- Maenhaut, W., I. Salma, J. Cafmeyer, H. J. Annegarn, and M. O. Andreae, Regional atmospheric aerosol composition and sources in the eastern Transvaal, South Africa, and impact of biomass burning, *J. Geophys. Res.*, 101, 23,631–23,650, 1996b.
- Martins, J. V., P. Artaxo, C. Lioussé, J. S. Reid, P. V. Hobbs, and Y. J. Kaufman, Effects of black carbon content, particle size, and mixing on light absorption by aerosol particles from biomass burning in Brazil, *J. Geophys. Res.*, this issue.
- Mason, B., *Principles of Geochemistry*, 3rd ed., John Wiley, New York, 1966.
- Nemeruyk, G. E., Migration of salts into the atmosphere during transpiration, *Sov. Plant Physiol.*, 17, 560–566, 1970.
- Penner, J. E., R. E. Dickinson, and C. A. O'Neil, Effects of aerosol from biomass burning on the global radiation budget, *Science*, 256, 1432–1434, 1992.
- Pereira, E. B., A. W. Setzer, F. Gerab, P. Artaxo, M. C. Pereira, and G. Monroe, Airborne measurements of biomass burning aerosols in Brazil related to the TRACE-A experiment, *J. Geophys. Res.*, 101, 23,983–23,992, 1996.
- Pielke, R. A., et al., A comprehensive meteorological modeling system—RAMS, *Meteorol. Atmos. Phys.*, 49, 69–91, 1992.
- Reid, J. S., and P. V. Hobbs, Physical and optical properties of young smoke from individual biomass fires in Brazil, *J. Geophys. Res.*, this issue.
- Reid, J. S., P. V. Hobbs, C. Lioussé, J. V. Martins, R. E. Weiss, and T. F. Eck, Comparisons of techniques for measuring shortwave absorption and the black carbon content of aerosols from biomass burning in Brazil, *J. Geophys. Res.*, this issue.
- Robock, A., Enhancement of surface cooling due to forest fire smoke, *Science*, 242, 911–913, 1988.
- Rogers, C. F., J. G. Hudson, B. Zielinska, R. J. Tanner, J. Hallett, and J. G. Watson, Cloud condensation nuclei from biomass burning, in *Global Biomass Burning: Atmospheric, Climatic, and Biospheric Implications*, edited by J. Levine, pp. 431–438, MIT Press, Cambridge, Mass., 1992.
- Setzer, A. W., and M. C. Pereira, Amazonia biomass burning in 1987 and an estimate of their tropospheric emissions, *Ambio*, 20, 19–22, 1991.
- Setzer, A. W., M. C. Pereira, and A. C. Pereira Jr., Satellite studies of biomass burning in Amazonia—Some practical aspects, *Remote Sens. Rev.*, 10, 91–103, 1994.
- Swap, R., M. Garstang, S. Macko, P. Tyson, W. Maenhaut, P. Artaxo, P. Kallberg, and R. Talbot, The long-range transport of southern African aerosols to the tropical South Atlantic, *J. Geophys. Res.*, 101, 23,777–23,792, 1996.
- Talbot, R. W., M. O. Andreae, H. Berresheim, P. Artaxo, M. Garstang, R. C. Harriss, K. M. Beecher, and S. M. Li, Aerosol chemistry during the wet season in central Amazonia: The influence of long-range transport, *J. Geophys. Res.*, 95, 16,955–16,970, 1990.
- Thurston, G. C., and J. D. Spengler, A quantitative assessment of source contributions to inhalable particulate matter pollution in metropolitan Boston, *Atmos. Environ.*, 19, 9–25, 1985.
- Van Grieken, R., P. Artaxo, P. Bernard, F. Bruynseels, P. Otten, H. Storms, and C. Xhoffer, Characterization of individual environmental particles in *Chemistry for Protection of the Environment, Studies in Environmental Sciences*, vol. 34, edited by L. Pawlowski, E. Mentasti, W. J. Lacy, and C. Sarzanini, Elsevier, New York, 1988.
- Van Grieken, R., C. Xhoffer, L. Wouters, and P. Artaxo, Microanalysis techniques for the characterization of individual environmental particles, *Anal. Sci.*, 7, 1117–1122, 1991.
- Yamasoe, M. A., Estudo da composição elementar e iônica de aerossóis emitidos em queimadas na Amazônia (in Portuguese), M.S. thesis, Inst. of Phys., Univ. of São Paulo, Brazil, 1995.

P. Artaxo, A. Castanho, E. T. Fernandes, K. M. Longo, J. V. Martins, M. A. Yamasoe, Instituto de Física, Universidade de São Paulo, Caixa Postal 66318, CEP 05315-970, São Paulo, Brazil. (e-mail: artaxo@if.usp.br)

P. V. Hobbs, Department of Atmospheric Sciences, University of Washington, Seattle, WA 98195-1640. (e-mail: phobbs@atmos.washington.edu)

W. Maenhaut, Institute for Nuclear Sciences, University of Ghent, Proeftuinstraat 86, B9000, Belgium. (e-mail: maenhaut@inwchem.rug.be.)

(Received September 10, 1997; revised July 1, 1998; accepted July 9, 1998.)